

# Identification of Adsorbed Phenyl ( $C_6H_5$ ) Groups on Metal Surfaces: Electron-Induced Dissociation of Benzene on Au(111)

Denis Syomin, Jooho Kim, and Bruce E. Koel\*

Department of Chemistry, University of Southern California, Los Angeles, California 90089-0482

G. Barney Ellison

Department of Chemistry & Biochemistry, University of Colorado, Boulder, Colorado 80309-0215

Received: May 31, 2001

We have investigated thermal and electron-induced chemistry of benzene ( $C_6H_6$ ) adsorbed on a Au(111) surface. Thermal desorption of benzene occurs in three desorption peaks: monolayer at 239 K, bilayer at 155 K, and multilayer films at 151 K. Electron-induced dissociation (EID) has been reported previously to selectively break a single C–H bond in molecules present in physisorbed layers and condensed films on metal surfaces, and we investigate whether EID at an incident energy of 30 eV can cleanly prepare adsorbed phenyl ( $C_6H_{5(a)}$ ) groups on the surface at low temperatures ( $\sim 90$  K). We use infrared reflection–absorption spectroscopy (IRAS) to show unequivocally that adsorbed phenyl groups can be formed by this procedure. Phenyl groups on Au(111) are bound with the molecular (ring) plane perpendicular to the Au surface plane, with the molecular  $z$ -axis tilted away from the surface normal. In contrast to previous reports of the chemistry of phenyl groups adsorbed on Cu(111) and Ag(111) surfaces, we find that adsorbed phenyl groups are stable only until 165 K on Au(111). At higher temperatures, phenyl groups undergo coupling reactions to form adsorbed biphenyl ( $C_6H_5-C_6H_5$ ) species which desorb intact from the surface at 400 K. While C–H activation (bond cleavage) on Au surfaces is difficult, hydrogenation and C–C coupling reactions are facile. Diffusion of aryl and alkyl intermediates to Au sites could result in immediate coupling and possibly desorption of products. This implies that Au atoms may play a more important role in bimetallic hydrocarbon conversion catalysis than simply blocking reactive sites.

## 1. Introduction

The formation of hydrocarbon fragments on metal surfaces is an important aspect of research in surface science because of the interest in studying catalytic reaction intermediates. An important fragment of benzene ( $C_6H_6$ ) is the phenyl radical ( $C_6H_5$ ). The formation and chemistry of adsorbed phenyl groups ( $C_6H_{5(a)}$ ) have been reported previously on Cu(111) and Ag(111) surfaces.<sup>1–7</sup> The experimental methods used to produce adsorbed phenyl groups may be divided into three groups: (i) thermal dissociation of adsorbed iodobenzene ( $C_6H_5I$ ), (ii) photon-stimulated dissociation of adsorbed  $C_6H_5I$  and chlorobenzene ( $C_6H_5Cl$ ), and (iii) electron-induced dissociation (EID) of adsorbed  $C_6H_6$  and  $C_6H_5Cl$ . Formation of  $C_6H_{5(a)}$  groups from thermal dissociation of  $C_6H_5I$  on a Cu(111) surface<sup>1–3</sup> was characterized with temperature-programmed desorption (TPD), high-resolution electron energy loss spectroscopy (HREELS), and H-atom titration experiments. It was proposed that phenyl groups were bound to the surface with the molecular (ring) plane tilted  $43 \pm 5^\circ$  away from the surface normal based on HREELS and near-edge X-ray absorption fine structure (NEXAFS) data. White and co-workers have also reported formation of phenyl groups bound to the Ag(111) surface by thermal and photon-induced dissociation of the C–I bond in  $C_6H_5I$  and EID of  $C_6H_6$ .<sup>6,7</sup> Formation of phenyl groups was indicated by reaction products of phenyl group coupling with coadsorbed methyl, ethyl, and phenyl fragments on the surface. No studies have been reported concerning  $C_6H_{5(a)}$  on Au surfaces.

Despite the fact that benzene adsorption has been extensively studied on many metal surfaces,<sup>8,10–15</sup> there is only one report concerning benzene–gold interactions.<sup>16</sup> Such information is important to a better understanding of the chemistry of bimetallic catalysts that contain Au. Such catalysts are used for selective hydrogenation and dehydrogenation, and other hydrocarbon conversion reactions. This motivates our studies of  $C_6H_{6(a)}$  and  $C_6H_{5(a)}$  chemistry on Au(111). These studies also provide comparisons to the benzene and phenyl surface chemistry on the other Group 1B metals of Cu and Ag, and information that is useful for the designed chemical modification of Au surfaces and the formation of interfaces between Au and organic solids involved in a variety of electrode contacts.

Vibrational spectroscopy offers the best opportunity for conclusively identifying isolation of  $C_6H_{5(a)}$ . Importantly, the infrared absorption spectra of  $C_6H_5$  radicals isolated in an Ar matrix at 12 K recently became available.<sup>17,18</sup> IR spectra of phenyl groups bonded to a metal center have also been reported for phenyltin<sup>19,20</sup> and phenylcopper<sup>21,22</sup> compounds. The only vibrational spectra reported to be from phenyl groups adsorbed on metal surfaces are from HREELS on Cu(111)<sup>1</sup> and IRAS on Cu(110).<sup>23</sup>

In this paper, we report TPD and IRAS studies of thermal and electron-induced chemistry of benzene adsorbed on a Au(111) surface. Adsorbed phenyl groups could be obtained by EID of a benzene monolayer and were identified and characterized by IRAS. The adsorption geometry of adsorbed benzene and phenyl groups on the surface was determined and the thermal chemistry of these species was investigated.

\* Corresponding author.

## 2. Experimental Methods

The experiments were performed in a UHV chamber described previously. The system had a base pressure of  $6 \times 10^{-10}$  Torr and was equipped for studies using Auger electron spectroscopy (AES), low energy electron diffraction (LEED), TPD, and IRAS. The Au(111) crystal could be resistively heated to 1000 K and cooled to 87 K by direct contact of liquid nitrogen with a copper block of the sample holder. The surface was cleaned by cycles of  $\text{Ar}^+$  ion sputtering (0.5 keV,  $6 \times 10^{-5}$  Torr) at 650 K for 10 min, and annealing at 1000 K for 20 min in UHV. This procedure resulted in a clean, well-ordered Au(111) surface with a LEED pattern corresponding to the known reconstruction of the Au(111) surface. No carbon or other contaminants were detected by AES.

Benzene ( $\text{C}_6\text{H}_6$ , Aldrich, 99+%) was degassed by several freeze–pump–thaw cycles before dosing. Gas dosing utilized a leak valve connected to a microcapillary-array doser, and was carried out with the Au(111) crystal at 87–90 K. TPD measurements were made with the sample placed in line-of-sight of the mass spectrometer ionizer at a location of 2 mm in front of the entrance aperture to a shield covering the ionizer. A heating rate of 3 K/s was used in TPD.

IRAS was carried out at grazing angles of  $86^\circ$ . An Infinity 60M FTIR spectrometer was used for collecting IR spectra. A medium-band, liquid-nitrogen cooled, mercury cadmium telluride (MCT) detector was used. Vibrational spectra were taken with the spectrometer resolution set to  $4\text{ cm}^{-1}$  and by averaging 1000 scans (5.5 min). All reported spectra were obtained with the sample at 87–90 K and ratioed against the clean Au(111) surface (as background).

EID experiments were performed using a variable-energy electron gun (5–1000 eV, Kimball Physics, Model FRA2x12). For this work, the incident electron beam energy was set to 30 eV and an incident beam current of  $10\text{ }\mu\text{A}$  was used, defocused over the crystal surface. The electron beam profile was measured in previous studies using a Faraday cup to have a full width at half-maximum equal to the crystal diameter, so that the flux varies across the surface by at most a factor of 2.

$\text{C}_6\text{H}_6$  coverages herein are referenced to  $\theta = 1$  monolayer (ML) for the  $\text{C}_6\text{H}_6$  coverage that corresponds to saturation of the most strongly bound  $\text{C}_6\text{H}_6$  TPD peak on Au(111). The  $\text{C}_6\text{H}_6$  exposure required to form this monolayer coverage was determined in TPD experiments.

## 3. Results

**3.1. Benzene ( $\text{C}_6\text{H}_6$ ) Adsorption and Thermal Chemistry on the Au(111) Surface.** Benzene is reversibly adsorbed on Au(111). A series of  $\text{C}_6\text{H}_6$  TPD spectra after  $\text{C}_6\text{H}_6$  exposures are shown in Figure 1. At a low coverage ( $\theta$ ) of roughly 0.1 monolayer (ML), benzene desorption occurs in a peak at 239 K as shown in the insert of Figure 1. A high-temperature shoulder can also be observed which we associate with desorption from defects. With increasing coverage, the desorption maximum shifts to lower temperature. A broad  $\text{C}_6\text{H}_6$  desorption feature occurs at 210 K after completion of the monolayer. At coverages exceeding one monolayer, two additional desorption peaks can be observed at 155 and 151 K and are assigned to desorption from the second layer and thicker films, respectively.

IRAS spectra of benzene adsorbed at several coverages on Au(111) are shown in Figure 2. Assignment of the IR bands to vibrational modes of adsorbed benzene is made on the basis of vibrational assignments of IR spectra for gas-phase benzene. These are shown in Table 1. At monolayer and lower coverages,

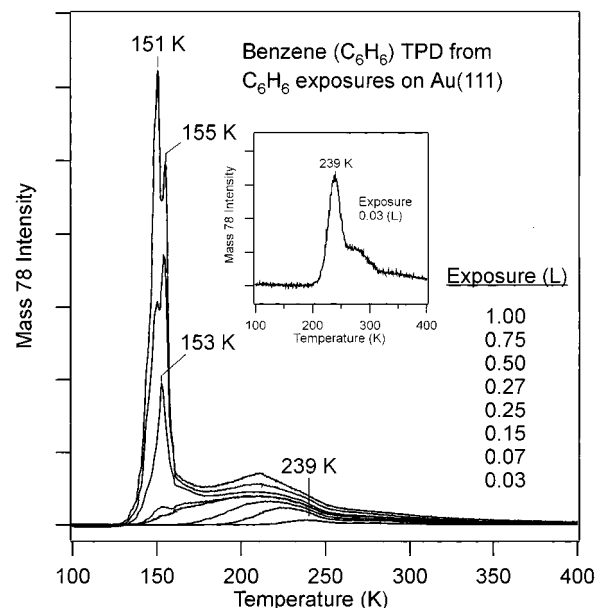


**Figure 1.**  $\text{C}_6\text{H}_6$  TPD spectra after  $\text{C}_6\text{H}_6$  exposures on Au(111) at 90 K.

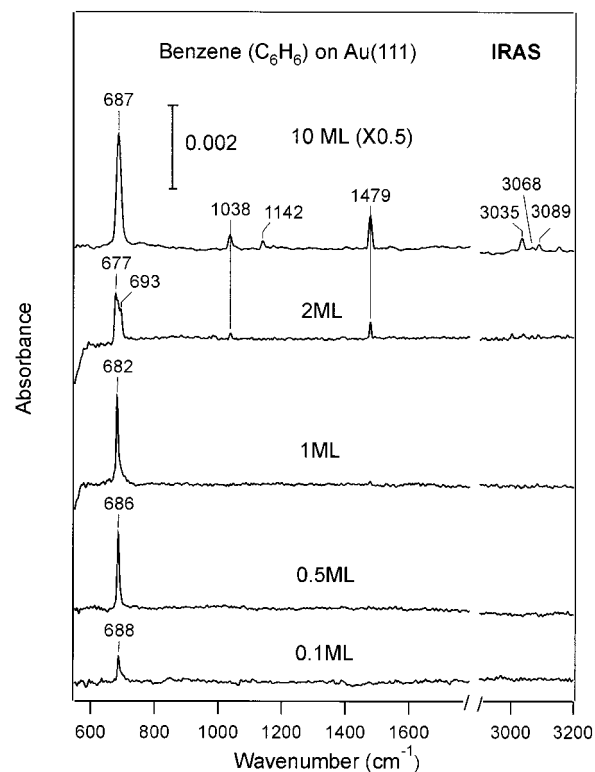


**Figure 2.** IRAS spectra of  $\text{C}_6\text{H}_6$  adlayers formed on Au(111) at 90 K.

only the C–H out-of-plane bending mode ( $\gamma\text{CH}$ ) at  $682\text{--}688\text{ cm}^{-1}$  was observed. Significant changes occur in the IR spectra of the benzene bilayer. First, two new bands, corresponding to C–H in-plane bending ( $\beta\text{CH}$ ) and ring stretching, appear in the spectra at  $1038$  and  $1479\text{ cm}^{-1}$ , respectively. Second, the  $\gamma\text{CH}$  band at  $682\text{ cm}^{-1}$  decreases in intensity, broadens, and splits into several peaks between  $677$  and  $693\text{ cm}^{-1}$ . For a 10-monolayer-thick film, bands are observed at  $687\text{ cm}^{-1}$  due to  $\gamma\text{CH}$ ,  $1038$  and  $1142\text{ cm}^{-1}$  due to  $\beta\text{CH}$ ,  $1479\text{ cm}^{-1}$  due to ring stretching, and  $3038$ ,  $3068$ , and  $3089\text{ cm}^{-1}$  due to C–H in-plane stretching ( $\nu\text{CH}$ ).

**3.2. Electron-Induced Chemistry of Benzene on the Au(111) Surface.** The TPD spectra shown in Figures 3 and 4

TABLE 1: Assignment of the IR Vibrational Spectra (cm<sup>-1</sup>) of Benzene Adsorbed on Au(111)<sup>a</sup>

repr. (D <sub>6h</sub> )	no.	type of mode	gas <sup>33</sup> phase	multilayer		monolayer			
				Au(111) (this work)	Cu(111) <sup>13</sup> (HREELS)	Au(111) (this work)	Ag(111) (HREELS)	Cu(111) <sup>13</sup> (HREELS)	Cu(110) <sup>14</sup>
a <sub>1g</sub>	ν <sub>1</sub>	νCH	3074	3068	3060				
	ν <sub>2</sub>	ring stretch	993						
a <sub>2g</sub>	ν <sub>3</sub>	βCH	1350						
a <sub>2u</sub>	ν <sub>4</sub>	γCH	674	687	675	682	675	685	685
b <sub>1u</sub>	ν <sub>5</sub>	νCH	3057	3089					
	ν <sub>6</sub>	ring deform	1010		1000				
b <sub>2g</sub>	ν <sub>7</sub>	γCH	990						
	ν <sub>8</sub>	ring deform	707						
b <sub>2u</sub>	ν <sub>9</sub>	ring stretch	1310						
	ν <sub>10</sub>	βCH	1148.5						
e <sub>1g</sub>	ν <sub>11</sub>	γCH	846		845				
e <sub>1u</sub>	ν <sub>12</sub>	νCH	3048						
	ν <sub>13</sub>	ring stretch and deform	1484	1479	1480				
	ν <sub>14</sub>	βCH	1038	1038					
	ν <sub>15</sub>	νCH	3057	3035					
e <sub>2g</sub>	ν <sub>16</sub>	ring stretch	1610		1595				
	ν <sub>17</sub>	βCH	1178	1142	1165				
e <sub>2u</sub>	ν <sub>18</sub>	ring deform	608						
	ν <sub>19</sub>	γCH	967						
	ν <sub>20</sub>	ring deform	398		410				

<sup>a</sup> ν stretch; β in-plane bend; γ out-of-plane bend.

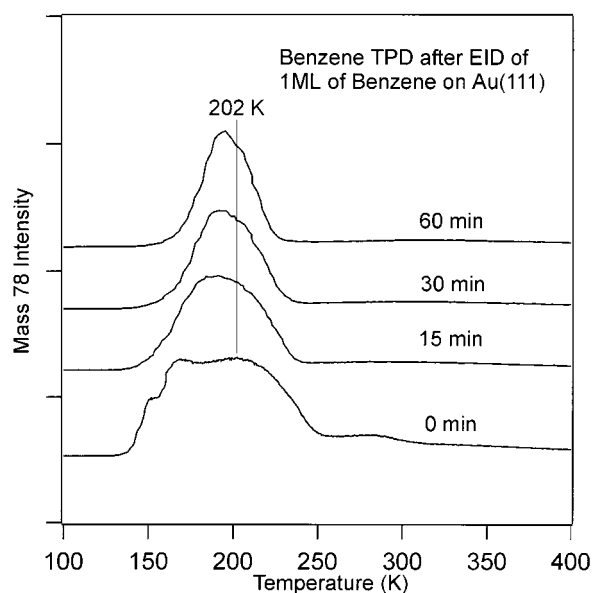


**Figure 3.** C<sub>6</sub>H<sub>6</sub> TPD spectra after a C<sub>6</sub>H<sub>6</sub> monolayer on Au(111) at 90 K was exposed to 30-eV electrons ( $I_i = 10 \mu\text{A}$  for 45 min to give  $2.14 \times 10^{17}$  electrons/cm<sup>2</sup>).

highlight changes that occur in the chemistry of benzene on Au(111) after exposing the benzene monolayer to 30-eV electrons. This caused the benzene desorption peak to be smaller and narrower, but did not cause any significant shift in the peak temperature as shown in Figure 3. Concurrently, a new TPD signal at 154 amu was detected, as shown in Figure 4, which was assigned to the desorption of biphenyl (C<sub>6</sub>H<sub>5</sub>–C<sub>6</sub>H<sub>5</sub>). There is no evidence of biphenylene, C<sub>6</sub>H<sub>4</sub>=C<sub>6</sub>H<sub>4</sub> (152 amu), which is a diagnostic for *o*-benzyne; this excludes *o*-C<sub>6</sub>H<sub>4</sub> as a EID product from benzene. The amount of biphenyl desorbed increased with increasing electron exposure, but the rate slowed with time.

IRAS spectra that probe the nascent changes in the benzene monolayer at 90 K after 30-eV electron exposure are also shown in Figure 5. The γCH band at 682 cm<sup>-1</sup> decreased in intensity

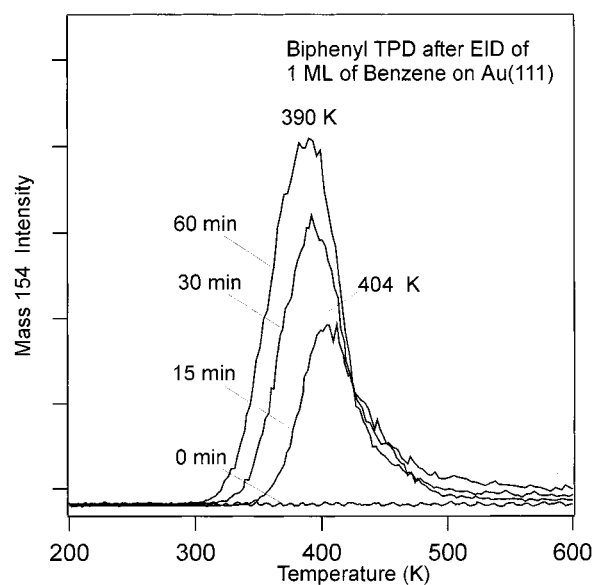


**Figure 4.** C<sub>12</sub>H<sub>10</sub> TPD spectra after a C<sub>6</sub>H<sub>6</sub> monolayer on Au(111) at 90 K was exposed to 30-eV electrons ( $I_i = 10 \mu\text{A}$  for 45 min to give  $2.14 \times 10^{17}$  electrons/cm<sup>2</sup>).

and new, small bands at 991, 1459, 1557, and 3055 cm<sup>-1</sup> appeared in the spectra following electron exposure.

To investigate the thermal chemistry of the products of EID, a “warm-up” study was performed in which the sample was heated sequentially to higher temperatures and IRAS spectra were taken at 90 K following each of these temperature excursions. The results are shown in Figure 6. Heating to 165 K caused the intensity of the γCH band at 682 cm<sup>-1</sup> to decrease, but had little effect on the intensity of the bands at 991, 1459, 1557, and 3055 cm<sup>-1</sup>. However, heating to 180 K caused these bands to nearly disappear, while the intensity of the γCH band at 682 cm<sup>-1</sup> remained unchanged. At the same time, two new bands at 693 and 731 cm<sup>-1</sup> appeared. Increasing the annealing temperature to 205 K decreased the intensity of the γCH band at 682 cm<sup>-1</sup> and eliminated any features at 991–3055 cm<sup>-1</sup>. Increasing the temperature further to 230 K caused the 682 cm<sup>-1</sup>

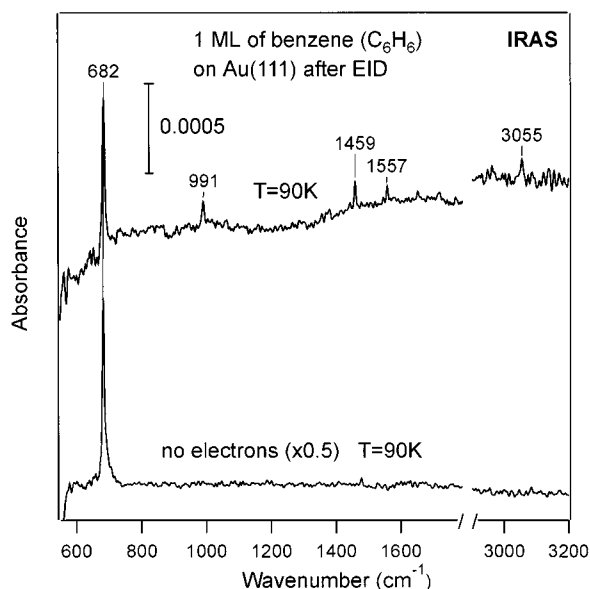


**Figure 5.** IRAS spectra of a  $C_6H_6$  monolayer on Au(111) at 90 K before and after exposure to 30-eV electrons ( $I_i = 10 \mu A$  for 45 min to give  $2.14 \times 10^{17}$  electrons/cm $^2$ ).

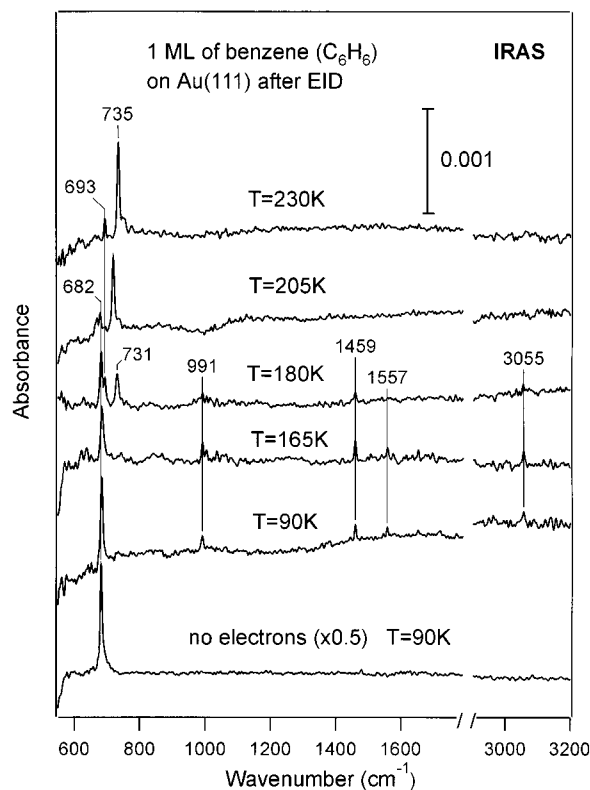


**Figure 6.** IRAS spectra after a  $C_6H_6$  monolayer on Au(111) at 90 K was exposed to 30-eV electrons ( $I_i = 10 \mu A$  for 45 min to give  $2.14 \times 10^{17}$  electrons/cm $^2$ ) and subsequently heated sequentially to higher temperatures.

band to disappear and an increase in intensity of the bands at 693 and 735  $cm^{-1}$ .

#### 4. Discussion

**4.1. Benzene Adsorption and Thermal Chemistry on Au(111) Surfaces.** It can be expected that benzene adsorption on Au(111) would be similar to that on Ag(111) and Cu(111). On Cu(111),<sup>13</sup> three  $C_6D_6$  desorption peaks were identified in TPD ( $\beta = 4$  K/s): (i) monolayer at 225 K ( $\theta \sim 0.1$  ML), (ii) bilayer

at 157 K, and (iii) multilayer at 152 K. Benzene molecules in the monolayer and in the first layer of the benzene bilayer on Cu(111) are oriented with their molecular (ring) plane approximately parallel to the surface, as determined by HREELS and NEXAFS. Strong intermolecular repulsive interactions were observed in TPD by a shift in the peak temperature near monolayer coverages. In the second layer of the benzene bilayer,  $C_6H_6$  molecules are oriented with their molecular planes perpendicular to the surface. In the benzene multilayer, benzene molecules were proposed to be randomly oriented. On Ag(111),  $C_6D_6$  was reported to desorb at 220 K ( $\theta \sim 0.25$  ML,  $\beta = 4$  K/s) from a chemisorbed state and at  $\sim 160$  K from a physisorbed state.<sup>5–7</sup>

Our TPD spectra following benzene adsorption on Au(111) are similar to those reported on Cu(111) and Ag(111). On Au(111), benzene is reversibly adsorbed, desorbing from the surface without any decomposition. The desorption peak for the monolayer shifts to lower temperatures consistent with first-order desorption kinetics, with repulsive lateral interactions lowering the desorption activation energy within the adsorbed monolayer. The desorption peak at 151 K did not saturate and shifts toward higher temperatures with increasing benzene exposures. This behavior and the shape of the peak is consistent with zero-order kinetics expected for desorption from a benzene multilayer. We assign the desorption peak at 155 K to desorption of the second benzene layer, as was done for benzene adsorption on Cu(111).

The desorption peak temperature for benzene ( $C_6D_6$ ) chemisorbed on Cu(111) is 225 K ( $\theta \sim 0.1$  ML and  $\beta = 4$  K/s), on Ag(111) is 220 K ( $\theta \sim 0.25$  ML and  $\beta = 4$  K/s), and on Au(111) is 239 K ( $\theta \sim 0.1$  ML and  $\beta = 3$  K/s). These data can be used with a simple Redhead analysis to estimate desorption energies of 13.3 and 14.7 kcal mol $^{-1}$  for Ag(111) and Au(111) surfaces, respectively. On Cu(111), the benzene adsorption energy was reported to be less than 14.3 kcal mol $^{-1}$ . We point out that benzene coverages of 0.1–0.25 ML were used to minimize the influence of surface defects at low coverages and repulsive interactions at high coverages. Our results show that benzene is more strongly bound to Au(111) than to Ag(111) or Cu(111). Nonetheless, the bonding in the monolayer on all three of these surfaces is much weaker than that on Ni(111), Pd(111), and Pt(111).<sup>10</sup> So, the benzene interaction with each of these Group 1B surfaces is basically the same, i.e., strong enough to orient the molecules adsorbed in the monolayer but not sufficient to activate the molecules for decomposition or reaction.

Benzene is nearly always adsorbed in the monolayer on metal surfaces in a “flat-lying” geometry with the molecular plane parallel to the surface.<sup>8,11,14,15,28</sup> The only exception to this reported in the literature is a tilted orientation for benzene on Pd(111).<sup>12</sup> For example, IRAS was used to deduce the orientation of benzene in the monolayer on Cu(110).<sup>14</sup> Only one absorption band at 685  $cm^{-1}$  corresponding to  $\gamma_{CH}$  was observed, and a flat-lying orientation was deduced on the basis of the surface selection rule. A single vibrational loss peak from the  $\gamma_{CH}$  mode of benzene on Cu(111) was observed in HREELS, indicating a flat-lying orientation at submonolayer coverages.

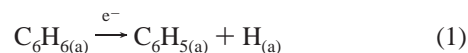
IRAS spectra of benzene adsorbed at submonolayer coverages on Au(111) are identical to the IR spectra of benzene adsorbed on Cu(111) and Cu(110). Using the surface selection rule and the relative intensities in the IR spectra of gas-phase benzene, we conclude that the orientation of benzene molecules at coverages up to one monolayer is with the molecular plane parallel to the surface.



Consistent with previous results on Cu(111) and Cu(110) surfaces, IRAS spectra of a two-monolayer benzene film on Au(111) is different from that of the monolayer. Several new vibrational bands from in-plane bending modes appear in the spectra and the  $\gamma$ CH band decreases in intensity, broadens, and splits into several peaks. This former observation can be explained by a change in orientation of the benzene molecules at this coverage: some of the molecules are adsorbed with their molecular plane tilted away from the surface plane. As a result, dynamic dipoles of in-plane bending and stretching modes of benzene are not screened by the metal surface and new bands appear in the spectra. IRAS averages over all molecules. Consequently, on the basis of only IRAS data, we cannot distinguish between the case where all benzene molecules are tilted away from the surface plane and where some of the molecules are parallel to the surface plane and some are tilted. Molecules in the second benzene layer desorb at a slightly higher temperature than do molecules in the multilayer. This means that the second benzene layer is slightly stabilized by the presence of the Au(111) surface in addition to the van der Waals forces operating within a condensed benzene phase. This may be due to a difference in orientation between the second and subsequent benzene layers. One possibility is that benzene molecules in the second layer are oriented selectively toward the surface plane in a tilted geometry, and not in a "T-shaped" structure present in the gas-phase dimer or crystalline solid.

The decrease in intensity of the  $\gamma$ CH band as the coverage of benzene exceeds one monolayer is similar to that observed on Cu(110).<sup>14</sup> This change in intensity and peak shape can be explained by a change in molecular orientation within the adlayer, i.e., tilting of benzene molecules in the chemisorbed monolayer away from the metal surface plane. A decrease would occur in the absorption cross section of the  $\gamma$ CH mode because of a smaller projection of the dynamic dipole moment for this mode on the surface normal. Also, tilting of benzene molecules in the chemisorbed layer would cause an asymmetry in the potential experienced by hydrogen atoms located at different positions within the molecule because of different interactions with the surface. This would produce different shifts of the  $\gamma$ CH band from the gas-phase value. We conclude that at least some fraction of the molecules in the chemisorbed monolayer change from a parallel to tilted orientation with respect to the surface plane as the coverage exceeds one monolayer. Second layer molecules are also tilted away from the surface plane. Multilayer molecules are more randomly oriented.

**4.2. Electron-Induced Dissociation (EID) of Benzene C<sub>6</sub>H<sub>6</sub> and the Identification of Adsorbed Phenyl C<sub>6</sub>H<sub>5(a)</sub> Groups on Au(111).** The experimental evidence for the selective formation of adsorbed phenyl groups on Au(111) by benzene EID



is that (i) C<sub>6</sub>H<sub>5</sub>–C<sub>6</sub>H<sub>5</sub> is the only hydrocarbon product (other than C<sub>6</sub>H<sub>6</sub>) remaining on, or evolved from, the surface by heating, and (ii) IRAS spectra to be further discussed below. Formation of biphenyl must be a result of C–C coupling reactions of adsorbed phenyl groups that are formed by selective, electron-induced cleavage of one C–H bond in benzene:



White and co-workers<sup>5–7</sup> concluded previously that EID can

be used to cleanly produce a monolayer of phenyl groups on the Ag(111) surface based on the biphenyl desorption product.

The other product of benzene EID is hydrogen. Recombination of H adatoms and desorption of H<sub>2</sub> from Au(111) occurs at 85–130 K,<sup>30</sup> and coadsorbed hydrocarbons should destabilize and lower this desorption temperature. We did not observe an H<sub>2</sub> TPD peak that was clearly resolved above the background or distinct from cracking of desorbing benzene. From this, hydrogen adatoms recombine and desorb as H<sub>2</sub> during EID at 90 K (this was not monitored), desorb as H<sub>2</sub> during TPD (in amounts too small to identify clearly), or hydrogenate phenyl groups to reform benzene during EID or TPD. In previous studies of adsorbed alkyl groups formed on Au(111) from the thermal dissociation of alkyl iodides, no H<sub>2</sub> evolution from the surface was detected in TPD, and so it was concluded that reductive elimination, in which an alkyl group is hydrogenated to form an alkane that desorbed promptly, was an extremely facile process. Similarly, we propose that a significant fraction of the H adatoms formed from benzene EID can hydrogenate phenyl groups to reform benzene during the EID process or at the onset of heating in TPD. This explains why the apparent cross section for EID was reduced after a decrease of only about 35% in the benzene desorption peak area after a 15-min electron exposure. This is in contrast to results for benzene EID on Ag(111),<sup>5</sup> where the apparent cross section for EID remained constant until over 60% of the benzene desorption peak was eliminated. This indicates that hydrogenation of phenyl groups on Au(111)



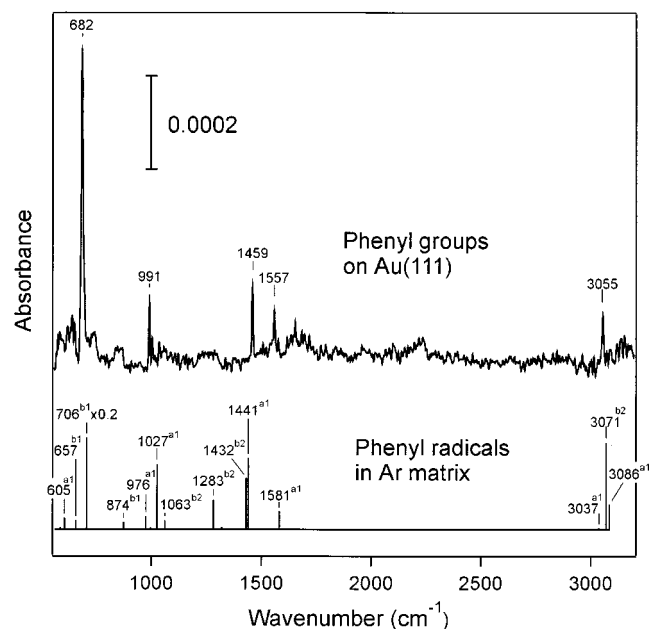
is a facile process, occurring at temperatures below 200 K.

Vibrational spectroscopy offers the best hope for actually identifying the surface species formed in the benzene monolayer after exposure to electrons in EID. We attribute the appearance of new vibrational bands at 3056 cm<sup>−1</sup> and in the 990–1500 cm<sup>−1</sup> region of the IR spectra to the formation of adsorbed phenyl groups, i.e., species that have formed a covalent, C<sub>6</sub>H<sub>5</sub>–Au  $\sigma$  bond to the surface. This assignment is made on the basis of comparisons to the infrared absorption spectra<sup>17</sup> of C<sub>6</sub>H<sub>5</sub> radicals isolated in an Ar matrix at 12 K and the IR spectra of phenyltin (Ph<sub>4</sub>Sn)<sup>19,20</sup> and phenylcopper (PhCu)<sup>21</sup> compounds in which phenyl groups are bonded to a metal center. To correlate peaks in the IR spectra of the adsorbed species on the Au(111) surface (Figure 6) with those of C<sub>6</sub>H<sub>5</sub> in an Ar matrix, we compare a spectral diagram for the phenyl radical with the IR spectra of the adsorbed layer in Figure 7. The phenyl radical spectral diagram was constructed from the position and intensity information reported in ref 18. The IR spectra for the adsorbate was obtained from summing four independent spectra that were each obtained in a manner identical to that for Figure 5.

Assuming that relative absorption cross sections for modes for the C<sub>6</sub>H<sub>5</sub> radical do not change significantly after adsorption on the gold surface, the mode at 991 cm<sup>−1</sup> might be assigned as  $\nu_7$ , of  $a_1$  symmetry, or as  $\nu_{26}$ , of  $b_2$  symmetry. The mode at 1459 cm<sup>−1</sup> can be assigned as  $\nu_5$  or as  $\nu_{22}$  and the feature at 1557 cm<sup>−1</sup> is identified as  $\nu_4$ . The mode at 3055 cm<sup>−1</sup> can be assigned as  $\nu_1$  or  $\nu_{19}$ . Table 2 summarizes this information along with our proposed vibrational assignment for the IRAS spectra of adsorbed C<sub>6</sub>H<sub>5</sub> groups on Au(111). For the phenyl radical, vibrational modes of symmetry type  $a_1$  and  $b_2$  correspond to in-plane modes and symmetry type  $a_2$  and  $b_1$  correspond to out-of-plane modes. All vibrational modes that we observed in the IR spectra of phenyl groups on the Au(111) surface are in-plane,  $a_1$  and  $b_2$  modes. The observation of in-plane vibrational modes

TABLE 2: Assignment of the IR Vibrational Spectra of Phenyl Radicals Adsorbed on Au(111)<sup>a</sup>

repr.	no.	type of mode	phenyl radical Ar matrix <sup>17</sup>	C <sub>6</sub> H <sub>5</sub> I <sup>35</sup> liquid	Ph <sub>4</sub> Sn <sup>19</sup>	PhCu <sup>21</sup>	adsorbed	
							Au(111) (this work)	Cu(111) <sup>1</sup> (HREELS)
a1	$\nu_1$	$\nu$ CH	3086					
	$\nu_2$	$\nu$ CH	3072					
	$\nu_3$	$\nu$ CH	3037	3031	3022			3020
	$\nu_4$	$\nu$ CC	1581	1577	1579	1586	1557	
	$\nu_5$	$\nu$ CC	1441	1468	1487	1470	1459	1470
	$\nu_6$	$\beta$ CCCH	1154	1175	1187	1162		1135
	$\nu_7$	$\nu$ CC	1027	1015	1027	1017–1020	991	
	$\nu_8$	ring breathing	997	997	997	985–990		995
	$\nu_9$	$\beta$ CCC	976					
	$\nu_{10}$	$\beta$ CC	605	653		672		
a2	$\nu_{11}$							
	$\nu_{12}$							
	$\nu_{13}$							
b1	$\nu_{14}$	$\gamma$ CH	972	984	978			
	$\nu_{15}$	$\gamma$ CH	874	904		906–912		880
	$\nu_{16}$	$\gamma$ CH	706	729		722–725		725
	$\nu_{17}$	$\gamma$ CH	657	681	685			
	$\nu_{18}$	$\gamma$ CH	416	448				
b2	$\nu_{19}$	$\nu$ CH	3071		3135		3055	
	$\nu_{20}$	$\nu$ CH	3060					
	$\nu_{21}$	$\nu$ CC	1624		1644			
	$\nu_{22}$	$\nu$ CC	1432	1435	1435	1416	1459	
	$\nu_{23}$	$\nu$ CC	1321	1321	1337			
	$\nu_{24}$	$\beta$ CCCH	1283	1259	1305			
	$\nu_{25}$	$\beta$ CCCH	1159	1159	1155	1126		
	$\nu_{26}$	$\beta$ CCCH	1063		1075	1055		
	$\nu_{26}$	$\beta$ CCC	587	613				

<sup>a</sup>  $\nu$  stretch;  $\beta$  in-plane bend;  $\gamma$  out-of-plane bend.

**Figure 7.** (Top) Average of four IRAS spectra after a C<sub>6</sub>H<sub>6</sub> monolayer on Au(111) at 90 K was exposed to 30-eV electrons ( $I_i = 10 \mu\text{A}$  for 45 min to give  $2.14 \times 10^{17}$  electrons/cm<sup>2</sup>) ((Bottom) Diagram of the IR spectra of the phenyl radicals in an Ar matrix. (The diagram was constructed using the positions and intensities reported for phenyl radicals in an Ar matrix.<sup>17</sup>)

in the IRAS spectra of adsorbed phenyl groups is clear evidence that these species are not oriented with the molecular plane parallel to the surface plane, as shown as the “parallel” orientation in Figure 8.

The intense  $\gamma$ CH band ( $\nu_{16}$ ) occurs at 706 cm<sup>-1</sup> for C<sub>6</sub>H<sub>5</sub> in an Ar matrix, 708 cm<sup>-1</sup> for phenyl groups in Ph<sub>4</sub>Sn, and 722–725 cm<sup>-1</sup> for the phenyl group in PhCu. On this basis, we expect a similar frequency of the  $\gamma$ CH mode of adsorbed phenyl groups

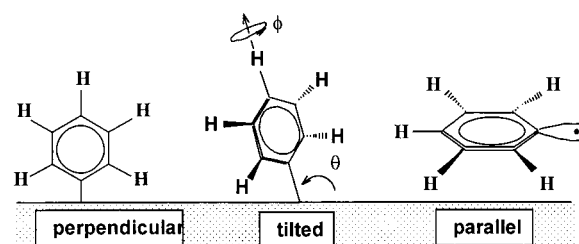
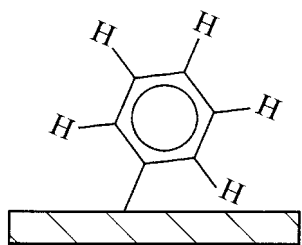


**Figure 8.** Schematic drawings of possible orientations of adsorbed phenyl groups on Au(111) surfaces.

on Au(111). The fact that such an intense vibrational mode is not observed in the IR spectra of adsorbed phenyl groups on Au(111) implies that the molecular plane is oriented perpendicular to the surface, as shown as the “perpendicular” orientation in Figure 8, and excludes the more general “tilted” model. (We attribute the intense absorption at 682 cm<sup>-1</sup> to the  $\gamma$ CH mode of benzene remaining on the surface after EID.) In this geometry, the dynamic dipole of the  $\gamma$ CH mode is screened by the surface. This conclusion is supported by the observation of an intense  $\gamma$ CH mode at 735 cm<sup>-1</sup> when adsorbed biphenyl species are formed, as shown in Figure 6. We assigned the top spectrum in Figure 6 to adsorbed biphenyl with bands at 693 and 735 cm<sup>-1</sup> from  $\gamma$ CH modes based on IRAS spectra of adsorbed biphenyl obtained by dosing gas-phase biphenyl on Au(111). It would be difficult to explain such a large change in the intensity of the  $\gamma$ CH mode simply by coupling of two phenyl groups without a large change in orientation of the two rings.

Accepting that phenyl groups adsorb with their molecular plane perpendicular to the surface, we still need to consider three possibilities for the adsorption geometry: (a)  $z$ -axis of the phenyl group aligned along the surface normal, as shown in Figure 8, (b)  $z$ -axis of the phenyl group tilted with respect to the surface normal, and (c)  $z$ -axis of the phenyl group aligned

## SCHEME 1



parallel to the surface plane but with the ring plane still perpendicular to the surface. Vibrational modes of  $a_1$  and  $b_2$  symmetry have dynamic dipole moments along the  $z$  and  $y$  (in-plane) molecular axis, respectively. According to the surface selection rule, only modes with  $a_1$  symmetry should be observed in IR spectra for a “perpendicular” orientation (Figure 8). If the  $z$ -axis of the phenyl group is tilted with respect to the surface normal, those modes which have  $a_1$  as well as  $b_2$  symmetry should be observed in the spectra. In the case of the  $z$ -axis of the phenyl group aligned parallel to the surface plane, only modes with  $b_2$  symmetry should be observed. Assignment of the  $\text{C}_6\text{H}_5$  mode at  $1557\text{ cm}^{-1}$  (Figure 6) to  $\nu_4$  of  $a_1$  symmetry allows us to exclude this latter orientation. This geometry also does not make sense chemically. If we assume a “perpendicular” orientation (with the  $z$ -axis of the phenyl group aligned along the surface normal), then all of the observed modes, including those at  $1459$  and  $3055\text{ cm}^{-1}$ , would have  $a_1$  symmetry. That means that bands at  $1459$  and  $3055\text{ cm}^{-1}$  in the spectra of adsorbed phenyl groups are correlated to modes of the phenyl radical at  $1441\text{ cm}^{-1}$  ( $\nu_5$ ,  $\nu_{\text{CC}}$ ) and at  $3086\text{ cm}^{-1}$  ( $\nu_1$ ,  $\nu_{\text{CH}}$ ), respectively. This is unlikely because the band at  $3086\text{ cm}^{-1}$  ( $\nu_1, a_1$ ,  $\nu_{\text{CH}}$ ) in the phenyl radical spectra from Figure 7 has almost three times lower intensity than the band at  $1441\text{ cm}^{-1}$  ( $\nu_5$ ,  $a_1$ ,  $\nu_{\text{CC}}$ ). In Figure 7, the intensity of the band at  $3055\text{ cm}^{-1}$  is 1.4 times smaller than the intensity of the band at  $1459\text{ cm}^{-1}$ . This difference in relative intensities exists despite the higher sensitivity of the MCT detector in the  $1400\text{ cm}^{-1}$  compared to the  $3000\text{ cm}^{-1}$  region. On the basis of this consideration, we exclude the “perpendicular” orientation. The remaining possibility is one with the ring plane perpendicular to the surface, but with a tilted  $z$  axis, as shown in Scheme 1.

Vibrational modes observed for adsorbed phenyl groups in this orientation can have  $a_1$  as well as  $b_2$  symmetry. This assignment is also consistent with the relative intensities of the bands in the IR spectra of phenyl radicals in an Ar matrix. We correlate the band at  $3055\text{ cm}^{-1}$  in adsorbed phenyl to that at  $3071\text{ cm}^{-1}$  ( $\nu_{19}$ ,  $b_2$ ,  $\nu_{\text{CH}}$ ) in phenyl radical, the band at  $1557\text{ cm}^{-1}$  in adsorbed phenyl to that at  $1581\text{ cm}^{-1}$  ( $\nu_4$ ,  $a_1$ ,  $\nu_{\text{CC}}$ ) in phenyl radical, and the band at  $991\text{ cm}^{-1}$  in adsorbed phenyl to that at  $1027\text{ cm}^{-1}$  ( $\nu_7$ ,  $a_1$ ,  $\nu_{\text{CC}}$ ) in the phenyl radical. We consider the band at  $1459\text{ cm}^{-1}$  in adsorbed phenyl to result from two unresolved bands correlated to those in  $\text{C}_6\text{H}_5$  at  $1441\text{ cm}^{-1}$  ( $\nu_5$ ,  $a_1$ ,  $\nu_{\text{CC}}$ ) and  $1432\text{ cm}^{-1}$  ( $\nu_{22}$ ,  $b_2$ ,  $\nu_{\text{CC}}$ ).

A change in the nature of the surface chemical bond between benzene and phenyl groups explains the large change in the orientation of the adsorbed species from “flat-lying” for  $\pi$ -bonded benzene to “upright” for  $\sigma$ -bonded phenyl groups.

**4.3. Phenyl Adsorption and Thermal Chemistry on Au(111) Surfaces.** Coupling of phenyl groups on Au(111) to form adsorbed biphenyl occurs at very low temperatures of  $165\text{ K}$ . This is in contrast to the temperatures required of at least  $300\text{ K}$  on Cu and Ag surfaces.<sup>1,7</sup> The  $\sigma$ -bond for phenyl adsorbed on Au(111) is very weak, as indicated by the value of  $D(\text{CH}_3\text{—Au}) = 22\text{ kcal mol}^{-1}$  estimated by calculations using density

functional theory (DFT). This helps to explain the small barrier required for bimolecular coupling. These results also illustrate that Au sites on bimetallic catalysts may be much more reactive than often discussed based on the weak activation of chemisorbed molecules by Au and its poor ability to catalyze C—H and C—C bond breaking. Diffusion of aryl and alkyl intermediates to Au sites could result in immediate coupling and possibly desorption of products.

As we established earlier, low coverages of biphenyl desorb above  $400\text{ K}$  following biphenyl dosing from the gas phase.<sup>31</sup> This is identical to the biphenyl desorption temperature following benzene EID experiments (Figure 4). Thus, biphenyl evolution after benzene EID is a desorption rate-limited process. This is consistent with our finding that phenyl coupling reactions occur at temperatures of  $\sim 165\text{ K}$  on Au(111).

The other product from the conversion of benzene to biphenyl via phenyl coupling reactions is hydrogen. The formation of every mole of biphenyl must be accompanied by the formation of 2 mol of H adatoms. However, since the amount of biphenyl that is desorbed only reaches a yield of  $0.25\theta^{\text{sat}}$ , ( $\theta^{\text{sat}}_{\text{C}_{12}\text{H}_{10}} = 0.084\text{ ML}$  defined relative to the Au surface atom density on Au(111)),<sup>31</sup> this corresponds to only  $0.02\text{ ML H}_2$ , and this small amount desorbs undetected either during EID or subsequent TPD.

## 5. Conclusion

Benzene is reversibly adsorbed on Au(111) and desorbs in three peaks: monolayer ( $T_p = 239\text{ K}$ ), bilayer ( $T_p = 155\text{ K}$ ), and multilayer ( $T_p \geq 151\text{ K}$ ). At submonolayer coverages, benzene is oriented with the molecular plane parallel to the Au(111) surface plane, and the chemisorption bond of  $\sim 14.7\text{ kcal mol}^{-1}$  is slightly stronger than on Ag(111) and Cu(111). Formation of thicker films converts part of the first-layer benzene to an orientation that is tilted away from the surface plane in a geometry similar to the second-layer molecules of the benzene bilayer. Multilayer benzene films contain molecules that are more randomly oriented with respect to the Au(111) surface plane.

Electron-induced dissociation of benzene on Au(111) produces chemisorbed phenyl groups on the surface, as identified by using IRAS. The adsorption geometry of phenyl groups was also determined to be with the molecular plane oriented perpendicular, and with the molecular  $z$ -axis tilted, to the Au(111) surface plane. Adsorbed phenyl groups are stable on the surface until  $165\text{ K}$ , where coupling occurs to produce chemisorbed biphenyl,  $\text{C}_6\text{H}_5\text{—C}_6\text{H}_5$ . The activation energy for this reaction is estimated to be  $10\text{ kcal mol}^{-1}$ . Biphenyl desorbs above  $400\text{ K}$  leaving a clean surface. This corresponds to a chemisorption bond energy of  $\sim 25\text{ kcal mol}^{-1}$ , and indicates that the barrier to breaking C—H bonds in aromatic molecules on Au(111) exceeds this value. While C—H activation (bond cleavage) on Au surfaces is difficult, hydrogenation and C—C coupling reactions are facile. Diffusion of aryl and alkyl intermediates to Au sites could result in immediate coupling and possibly desorption of products. This implies that Au atoms may play a more important role in bimetallic hydrocarbon conversion catalysis than simply blocking reactive sites.

**Acknowledgment.** B.E.K. acknowledges support of this work by the ACS Petroleum Research Foundation. G.B.E. is a Fellow of the J. S. Guggenheim Foundation.

## References and Notes

- (1) Xi, M.; Bent, B. E. *Surf. Sci.* **1992**, 278, 19.
- (2) Xi, M.; Bent, B. E. *J. Am. Chem. Soc.* **1993**, 115, 7426.

- (3) Xi, M.; Bent, B. E. *Langmuir* **1994**, *10*, 505.  
(4) Zhou, X.-L.; White, J. M. *J. Chem. Phys.* **1990**, *92* (9), 5612.  
(5) Zhou, X.-L.; Castro, M. E.; White, J. M. *Surf. Sci.* **1990**, *238*, 215.  
(6) Zhou, X.-L.; Schwaner, A. L.; White, J. M. *J. Am. Chem. Soc.* **1993**, *115*, 4309.  
(7) White, J. M. *Langmuir* **1994**, *10*, 3946.  
(8) Yang, M. X.; Xi, M.; Yuan, H.; Bent, B. E.; Stevens, P.; White, J. M. *Surf. Sci.* **1995**, *341*, 9, and references therein.  
(9) Szulczewski, G. J.; White, J. M. *Surf. Sci.* **1998**, *399*, 305.  
(10) Netzer, F. P. *Langmuir* **1991**, *7*, 2544, and references therein.  
(11) Yannoulis, P.; Dudde, R.; Frank, K. H.; Koch, E. E. *Surf. Sci.* **1987**, *189/190*, 519.  
(12) Hoffman, H.; Zaera, F.; Ormerod, R. M.; Lambert, R. M.; Wang, L. P.; Tysoe, W. T. *Surf. Sci.* **1990**, *232*, 259.  
(13) Xi, M.; Yang, M. X.; Jo, S. K.; Bent, B. E.; Stevens, P. *J. Chem. Phys.* **1994**, *101*, 9122.  
(14) Haq, S.; King, D. A. *J. Phys. Chem.* **1996**, *100*, 16957.  
(15) Kang, J.-H.; Toomes, R. L.; Robinson, J.; Woodruff, D. P.; Schaff, O.; Terborg, R.; Lindsay, R.; Baumgartel, P.; Bradshaw, A. M. *Surf. Sci.* **2000**, *448*, 23.  
(16) Wetteree, S. M.; Lavrich, D. J.; Cummings, T.; Bernasek, S. L.; Scoles, G. *J. Phys. Chem. B* **1998**, *102*, 9266.  
(17) Radziszewski, J. G.; Nimlos, M. R.; Winter, P. R.; Ellison, G. B. *J. Am. Chem. Soc.* **1996**, *118*, 7400.  
(18) Friderichsen, A. V.; Radziszewski, J. G.; Nimlos, M. R.; Winter, P. R.; Dayton, D. C.; David, D. E.; Ellison, G. B. *J. Am. Chem. Soc.* **2001**, *123*, 1977.  
(19) Griffiths, V. S.; Derwish, J. A. *J. Mol. Spectrosc.* **1960**, *2*, 148.  
(20) Poller, R. C. *J. Inorg. Nucl. Chem.* **1962**, *24*, 593.  
(21) Costa, G.; Camus, A.; Gatti, L.; Marsich, N. *J. Organomet. Chem.* **1966**, *5*, 568.  
(22) Costa, G.; Camus, A.; Marsich, N.; Gatti, L. *J. Organomet. Chem.* **1967**, *8*, 339.  
(23) Chen, Q.; Haq, S.; Freederick, B. G.; Richardson, N. V. *Surf. Sci.* **1996**, *368*, 310.  
(24) Wang, J.; Koel, B. E. *J. Phys. Chem.* **1998**, *102*, 8573.  
(25) Van Hove, M. A.; Koestner, R. J.; Stair, P. C.; Biberian, J. P.; Kesmodel, L. L.; Bartos, I.; Somorjai, G. A. *Surf. Sci.* **1981**, *103*, 189.  
(26) Tsai, Y.-L. Ph.D. Thesis, University of Southern California, 1996.  
(27) Radziszewski, J. G.; Hess, B. A., Jr.; Zahradnik, R. *J. Am. Chem. Soc.* **1992**, *114*, 52.  
(28) Koel, B. E.; Crowell, J. E.; Mate, C. M.; Somorjai, G. A. *J. Phys. Chem.* **1984**, *88*, 1988.  
(29) Hayden, B. E. In *Vibrational Spectroscopy of Molecules on Surfaces*; Yates, J. T., Jr., Madey, T. E., Eds.; Plenum Press: New York, 1987; p 267.  
(30) Paul, A.; Yang, M. X.; Bent, B. E. *Surf. Sci.* **1993**, *297*, 327.  
(31) Syomin, D.; Koel, B. E. *Surf. Sci.*, in press.  
(32) Mavrikakis, M. Personal communications.  
(33) Dang-Nhu, M.; Pliva, J. *J. Mol. Spectrosc.* **1989**, *138*, 423.  
(34) Avouris, P.; Demuth, J. E. *J. Chem. Phys.* **1981**, *75*, 4783.  
(35) Sverdlov, L. M.; Kovner, M. A.; Krainov, E. P. *Vibrational Spectra of Polyatomic Molecules*; John Wiley & Sons: New York, 1974.